Topological insulator laser : theory

Chong, Yi Dong; Harari, Gal; Bandres, Miguel A.; Lumer, Yaakov; Rechtsman, Mikael C.; Khajavikhan, Mercedeh; Christodoulides, Demetrios N.; Segev, Mordechai

2018

Harari, G., Bandres, M. A., Lumer, Y., Rechtsman, M. C., Chong, Y. D., Khajavikhan, M., . . . Segev, M. (2018). Topological insulator laser : theory. Science, 359(6381), eaar4003-. doi:10.1126/science.aar4003

https://hdl.handle.net/10356/90137

https://doi.org/10.1126/science.aar4003

Topological Insulator Laser

Part I: Theory

Gal Harari[1+], Miguel A. Bandres[1+], Yaakov Lumer[2], Mikael C. Rechtsman[3], Y. D. Chong[4], Mercedeh Khajavikhan[5], Demetrios N. Christodoulides[5] and Mordechai Segev[1*]

1. *Physics Department and Solid State Institute, Technion, Haifa 32000, Israel*
2. *Department of Electrical and Systems Engineering, University of Pennsylvania, Philadelphia, PA 19104, USA*
3. *Department of Physics, The Pennsylvania State University, University Park, PA 16802, USA*
4. *Division of Physics and Applied Physics, Nanyang Technological University, Singapore 637371, Singapore*
5. *CREOL, College of Optics and Photonics, University of Central Florida, Orlando, FL 32816, USA*

+ Equal contribution authors
**msegev@tx.technion.ac.il*

Topological insulators are phases of matter characterized by topological edge states that propagate in a unidirectional manner that is robust to imperfections and disorder. These attributes make topological insulator systems ideal candidates for enabling applications in quantum computation and spintronics. Here, we propose a fundamentally new approach in exploiting topological effects in a unique way: the topological insulator laser. These are lasers whose lasing mode exhibits topologically-protected transport without magnetic fields. We show that the underlying topological properties lead to a highly efficient laser, robust to defects and disorder, with single mode lasing even at very high gain values. The proposed concept alters current understanding of the interplay between disorder and lasing, and at the same time opens exciting possibilities in topological physics, such as topologically-protected transport in systems with gain. On the technological side, the topological insulator laser offers an avenue to make many semiconductor lasers to operate as a single-mode high-power laser, while coupled efficiently into an output port.

Topological insulators emerged in condensed matter physics [1–3], and constitute a new phase of matter, with insulating bulk and quantized and robust edge conductance. The prospect of observing topological effects in non-electronic systems was first proposed and demonstrated in microwaves in gyro-optic crystals with broken time-reversal symmetry [4–6]. The transition to optical frequencies required another conceptual leap. Theoretical proposals [7–10] were followed by the first two experiments utilizing artificial gauge fields, one based on a honeycomb lattice of helical waveguides [11], and the other based on an array of aperiodic coupled silicon microring resonators [12]. To date, topological protection is known to be a ubiquitous phenomenon, occurring in many physical settings, ranging from photonics [6,11–16] and cold atoms [17,18] to acoustic, mechanical and elastic systems [19–22]. So far, however, most of these activities were carried out in entirely passive, linear, and conservative settings.

Lasers, on the other hand, represent complex, non-conservative systems capable of exhibiting very rich dynamics. They are fundamentally non-Hermitian and non-linear entities that rely on saturable gain. Introducing non-Hermiticity to topological systems raises fundamental questions on whether non-Hermitian topological systems can exist at all [23], and if they do – how to define the topological phases and their stability [24]. Part of this controversy has recently been resolved, and it is now known that one-dimensional non-Hermitian systems can have stationary zero-dimensional topological edge states [25,26] and topological defect states [27–29], and these can even lase [29–32]. However, being one-dimensional systems lasing from a localized defect, none of these systems can support transport via edge states. Very recently, lasing from a topological edge state in a photonic crystal subject to an external magnetic field – a photonic-analogue of the quantum Hall effect – was demonstrated [33]. That system employed magneto-optic effects, which are very weak at optical frequencies, and accordingly only a narrow topological bandgap (40pm) within which lasing occurred [33]. Clearly, would be important to pursue new approaches in

expanding the topological photonic bandgap, and hence the degree of protection endowed to such structures. Equally important, in terms of applications, will be to follow an all-dielectric strategy that is by nature compatible with semiconductor laser technologies.

Notwithstanding recent progress in topological photonics and lasing therein, the fundamental question is still open: can topological protection of transport be employed in non-Hermitian, highly nonlinear, open systems such as lasers? Addressing this issue is at the heart of the topological insulator laser, along with many new questions, such as, can a topological insulator include gain – which has no equivalent in condensed matter physics? What happens to the stimulated emission under topologically-protected transport? Perhaps the most important question here is: can a topological insulator laser exist without magnetic field, and if it does, can it exhibit new features, and profoundly improved laser action?

Laser cavities are typically optimized to attain high Q-factors, and they are always strongly affected by disorder, should it arise from manufacturing imperfections, operational failure, stresses, etc. A prominent consequence of disorder is mode localization, which has dire implications in photonics [34,35]. To a laser, disorder implies degraded overlap of the lasing mode with the gain profile, lower output coupling and multimode lasing, altogether resulting in an overall reduced efficiency. These problems are further exacerbated in more involved arrangements such as laser arrays. Such laser array structures tend to lase with many modes simultaneously, with their modal structure (near field and spectrum) varying with the pumping strength. Despite many methods suggested to control the emission pattern of laser diode arrays, they are mostly used as pumps for solid state lasers.

Here, we introduce topological insulator lasers: lasers whose lasing mode exhibits topologically-protected transport, such that the light propagates along the edges of the cavity in a unidirectional fashion, immune to scattering and disorder, unaffected by the shape of the edges. We show that the underlying topological properties lead to a highly efficient laser, robust to fabrication and

operational disorder and defects, and single-mode lasing even at gain values high above the laser threshold. The proposed topological insulator laser alters the current understanding of laser systems and opens a new realm of study of topological insulators in active media.

To demonstrate the concept underlying topological insulator lasers, we consider two possible configurations involving planar arrays of coupled, active resonators. The first is based on the Haldane model [18,36] — an archetypical model for time-reversal-broken topological insulators. The second relies on an aperiodic array architecture that creates an artificial magnetic field, as was demonstrated experimentally in passive systems (silicon) [8,12,13,37]. **This is an all-dielectric system, which has been realized with current semiconductor laser technology – as described in the accompanying experimental paper (Topological Insulator Laser Part II: Experiments).**

In the Haldane design [36], the resonators of the topological insulator laser are arranged in a honeycomb lattice, as shown in Fig. 1a. Each resonator is coupled to its nearest neighbors by a real hopping parameter t_1, and to its second neighbors by a complex parameter $t_2 \exp(i\phi)$ (see SI). The two sublattices of the honeycomb structure have identical on-site potentials. The passive Haldane model (no gain or loss, but $t_2 \neq 0$) exhibits two phases: the trivial phase when ϕ (the Haldane flux parameter) is equal to 0 or π, and the topological phase when $\phi \neq 0, \pi$. In the topological phase, edge states emerge with energies extending across the topological gap that is proportional to $t_2 \sin(\phi)$, reaching a maximum at $\phi = \pi/2$. To promote the lasing of the topological edge mode, we specifically design the honeycomb array to have zig-zag edges that have small penetration depth into the bulk. The evolution of the field of this laser system is governed by

$$i\frac{\partial \vec{\psi}}{\partial t} = H_{Haldane}\vec{\psi} - i\gamma\vec{\psi} + \frac{ig\mathbb{P}}{1+|\vec{\psi}|^2/I_{sat}}\vec{\psi} + H_{output}\vec{\psi}, \quad (1)$$

where $\vec{\psi}$ is a column vector encompassing the modal amplitudes of the array elements, $H_{Haldane}$ is the standard Haldane Hamiltonian (see SI), which depends on the resonance frequency of a single resonator ω_0, the hopping constants, $t_{1,2}$, and the Haldane flux ϕ. Here, γ represents the loss in

each resonator, and is assumed to be linear loss (as in all CW lasers), although we simulated saturable loss as well, and our results are effectively the same. The third term in Eq. (1) represents optical gain via stimulated emission that is inherently saturable (I_{sat}). Here, $\mathbb{P}$ stands for the spatial profile of the pump, and H_{output} describes the output coupler (a semi-infinite chain of resonators), which is what makes this an open system, and its coupling to the cavity. To promote lasing of the edge modes, the gain (g) is provided only to the resonators on the perimeter, as depicted in Fig. 1a. In general, g is a function of the frequency; however, in semiconductors the gain is broadband (compared to the inter-ring coupling constant), hence it is assumed to be frequency-independent.

We study the topological insulator laser by simulating the full dynamics and by directly solving for the nonlinear lasing modes of Eq. (1) (see SI). We consider two cases: (i) a trivial arrangement where $\phi = 0$, and (ii) a topological array when the Haldane flux is $\phi = \pi/2$. In the trivial case ($\phi = 0$), even without disorder, the first lasing mode is localized away from the output coupler, as shown in Fig. 2d, so as to minimize the power loss through the coupler. This strongly affects the lasing efficiency because the localized lasing mode does not use all the gain available around the perimeter and it is coupled only very weakly to the output. This adversarial effect is further enhanced in the presence of disorder given that it tends to highly localize modes. For example, as shown in Fig. 2e, in the presence of disorder, the lasing mode of the trivial cavity becomes further confined within just a few resonators. Finally, since the trivial lasing mode does not spatially deplete the gain, if pumped harder, multiple modes can reach threshold, giving rise to multimode operation, as shown in Fig. 3f.

On the other hand, in the topological case ($\phi = \pi/2$), the lasing mode possesses all the distinct characteristics of topological chiral edge states: it is extended all around the perimeter of the cavity with almost-uniform intensity, and its energy flux is unidirectional. The unidirectionality of the energy flux can be observed in Fig. 1b by noticing how the energy starts accumulating while moving clockwise around the perimeter of the array, and then abruptly drops after the output

coupler. Even though the notion of topological invariants in non-Hermitian, non-linear open systems such as a laser, is still largely unexplored territory, one can recognize the topological nature of this array by observing its dynamics. In this regard, it is instructive to monitor the evolution in the system, starting from below transparency to lasing. In Fig. 3c-d, we show the behavior of the complex frequency of the cavity modes as we increase the gain from zero to the threshold level. During this process, the frequency (real part) of each mode is virtually unchanged, equal to the eigenfrequencies of the closed Hermitian system (the topological insulator lattice), and the band gap of the topological system (blue region in Fig 3a) remains well defined and constant. Clearly, the topological band gap does not close in the presence of gain (even high above the threshold level), and no topological phase transition occurs. This is a clear indication that the system retains its topological features even when it lases. More importantly, as shown in Fig. 3c, one of the topological edge modes is the first in line to lase. Moreover, we emphasize that even when we increase the gain (pumping) high above the threshold level, the lasing remains in a single-mode – the topological edge mode. This is because the topological lasing mode has almost uniform intensity all around the perimeter of the array, saturating the whole gain medium, hence suppressing all the other cavity modes and preventing them from lasing (Fig 3e).

To further examine the topological properties of the lasing mode, we study the system in the presence of disorder and defects. We find that even in the presence of disorder, the topological insulator laser still operates in a topological edge mode, as shown in Fig. 2b. Even when a defect is introduced – for example, a malfunctioning microring at the perimeter - the topological edge mode is able to bypass the defect with minimal penetration into the bulk (Fig. 2c).

It is instructive to highlight the role of topology in this topological insulator laser by comparing its efficiency to its trivial counterpart. The efficiency of lasers is universally defined by the so-called “slope efficiency”: the slope of the function describing the output power as a function of gain above the threshold level. Figure 4a shows the calculated slope efficiencies (in steady-state)

as a function of the strength of the disorder. When the cavity is in the trivial phase, $\phi = 0$, the slope efficiency is poor and further decreases in the presence of disorder. In sharp contrast, when the laser is topological, $\phi = \pi/2$, the lasing is very efficient and robust – it has a high slope efficiency (with a small variance) that remains high even at significant disorder levels. The topological protection ceases only when the strength of disorder is comparable to the size of the topological band gap. To reaffirm that the high efficiency of this laser is due to its topological protection, we evaluate the slope efficiency for structures with a smaller band gap, e.g. for $\phi = \pi/8$. As seen in Fig 4a, the slope efficiency of this "small topological gap implementation" is initially high, but when the level of disorder is increased – it deteriorates much faster than the $\phi = \pi/2$ case, because the disorder closes the smaller topological gap more easily. To further highlight the robustness of our topological insulator laser, we calculate the mean value of the slope efficiency as a function of disorder strength and the two main parameters that control the size of the topological band gap: the Haldane flux (Fig. 4b), and the second nearest neighbor coupling t_2 (Fig. 4c). As shown in Fig. 4(b-c), when the strength of randomness is less than the size of the Haldane topological band gap ($6\sqrt{3}t_2 \sin(\phi)$), the slope efficiency stays high, and just drops when the disorder level is bigger than the size of the topological band gap. This is a clear indication that the efficiency and robustness of the topological insulator laser stems from its topological properties[1].

Next, we study lasing in an aperiodic topological array of micro-ring resonators, which was one of the two platforms first explored for realizing photonic topological insulators [8,12]. This arrangement involves a lattice of coupled resonators with aperiodic couplers (schematically shown in SI)- an architecture that can be implemented using standard semiconductor technologies [38,39].

[1] For completeness, we also study the operation of the laser when the same system has a trivial gap, with no edge states crossing the gap. To open a trivial gap, we detune the resonance frequencies of the resonators associated with the two sublattices of the Haldane model. When the detuning is large enough, it opens a topologically-trivial bandgap even with $\phi = \pi/2$. We find that - only when the gap is topological - the efficiency of the laser is high and robust to disorder.

Importantly – this system does not employ magnetic fields, nor does it use any exotic materials (such as YIG). It relies on current semiconductor laser technology, and only that. The aperiodic couplers establish an artificial gauge field, thus leading to behavior analogous to the quantum Hall effect [12]. Since in the linear regime the system is reciprocal, both the clockwise (CW) and counterclockwise (CCW) modes in each microring resonator experience gauge fields with opposite signs. This, in turn, makes the overall cavity degenerate, i.e. for any frequency supported by the CW modes there is a corresponding CCW mode. In passive settings (no gain/loss), for reasonable experimental parameters, one can consider the CW and CCW as decoupled [8,12]. For a topological insulator laser based on this system, one must take into account that the CW and CCW modes inevitably interact with one another through the nonlinear effect of gain saturation and backscattering which naturally occur in active media [40].

This topological aperiodic laser array is simulated using an extended version of Eq.1 (see SI). To account for a realistic set-up in current semiconductor laser technology, we implement saturable gain and explicit coupling between the CW and CCW modes through the saturable medium and backscattering. We use the parameters of recent experiments [39] and of the accompanying experimental paper, which yield a topological bandgap of ~1nm, in an aperiodic ring array made of all-dielectric semiconductor laser materials. A topological gap of this size ensures very high topological protection of transport in the laser cavity. We essentially observe the same features as in the Haldane model: the topological lasing mode is extended, uniform, and couples strongly to the output coupler, even in the presence of disorder. In contrast, the topologically-trivial aperiodic array, having no edge modes, suffers from localization of its lasing modes, strong multimode lasing, and displays low output coupling (see Fig.5). It is important to stress that despite the reciprocity of the system and the inherent degeneracy of every ring and the presence of scattering and saturable gain (which cause lasing in both CW and CCW directions), the topologically-protected features of the lasing modes prevail, and the efficiency of the topological array is much

higher than that of the trivial case. The underlying mechanism can be clearly seen from the mode shapes in Fig. 5(b-e), where the mutual contribution of the two counterpropagating (CW and CCW) edge modes, with the same temporal frequency, depletes the gain and enforces efficient single-frequency lasing. In a similar vein, the topological lasing modes exhibit high robustness against defects and disorder, despite the backscattering and the nonlinear coupling between the CW and the CCW modes.

In conclusion, we introduced a new class of lasers that operate in a topological phase and take advantage of topologically-protected transport. Thanks to its topological properties, the topological insulator laser exhibits high efficiency, extreme robustness to defects and disorder, and single mode lasing even at gain levels high above the threshold. On the fundamentals side, the interplay between topology and non-Hermiticity, especially in nonlinear open system such as lasers, raises many fundamental questions. We showed here that the laser system based on the archetypal Haldane model exhibits topologically-protected transport, with features similar to its passive counterpart. This means that there must be associated topological invariants, in spite of the fact that this system is non-Hermitian. The implications of topologically-protected transport to lasing systems can change existing paradigms by harnessing the topological features of the lasing mode to yield high efficiency lasing single-mode lasing even high above threshold. What we proposed here is a proof of concept, not attempting to optimize the integration of topological properties into a laser. The topological design of the laser cavity can take on many different concrete designs, which may lead to new ideas and innovative applications. For example, the topological system can be based on topological network models of strongly-coupled resonators [41], which can be realized with very small units. More generally, new geometries, wherein a narrow linewidth gain medium is matched to the topological gap can be considered. In a similar vein, topological insulator lasers could be designed from flexible gain media (organics), and sustain distortions, manipulations, and perhaps also extreme conditions. Looking several steps

ahead, it may be possible to integrate topological insulator lasers with sensors, antennas and other photonic devices. The accompanying experimental paper describes the first realization of a topological insulator laser without magnetic field. It is an all-dielectric system, based on the aperiodic array of ring resonators described here fabricated with ordinary technology for making semiconductor lasers.

References

1. C. L. Kane and E. J. Mele, “Quantum Spin hall effect in graphene,” Phys. Rev. Lett. **95**, 226801 (2005).
2. B. A. Bernevig, T. L. Hughes, and S.C. Zhang, “Quantum Spin Hall Effect and Topological Phase Transition in HgTe Quantum Wells,” Science **314**, 1757 (2006).
3. M. König, S. Wiedmann, C. Brüne, A. Roth, H. Buhmann, L. W. Molenkamp, X. Qi, and S. Zhang, “Quantum Spin Hall Insulator State in HgTe Quantum Wells,” Science **318**, 766 (2007).
4. S. Raghu and F. Haldane, "Analogs of quantum-Hall-effect edge states in photonic crystals," Phys. Rev. A **78**, 033834 (2008).
5. Z. Wang, Y. D. Chong, J. D. Joannopoulos, and M. Soljačić, "Reflection-Free One-Way Edge Modes in a Gyromagnetic Photonic Crystal," Phys. Rev. Lett. **100**, 013905 (2008).
6. Z. Wang, Y. D. Chong, J. D. Joannopoulos, and M. Soljacić, “Observation of unidirectional backscattering-immune topological electromagnetic states.,” Nature **461**, 772 (2009).
7. R. O. Umucalılar and I. Carusotto, "Artificial gauge field for photons in coupled cavity arrays," Phys. Rev. A **84**, 043804 (2011).
8. M. Hafezi, E. Demler, M. Lukin, and J. Taylor, "Robust optical delay lines via topological protection," Nat. Phys. **7**, 9 (2011).
9. K. Fang, Z. Yu, and S. Fan, “Realizing effective magnetic field for photons by controlling the phase of dynamic modulation,” Nat. Photonics **6**, 782 (2012).
10. A. B. Khanikaev, S. Hossein Mousavi, W.-K. Tse, M. Kargarian, A. H. MacDonald, and G. Shvets, “Photonic topological insulators,” Nat. Mater. **12**, 233 (2012).
11. M. C. Rechtsman, J. M. Zeuner, Y. Plotnik, Y. Lumer, D. Podolsky, F. Dreisow, S. Nolte, M. Segev, and A. Szameit, “Photonic Floquet topological insulators.,” Nature **496**, 196 (2013).
12. M. Hafezi, S. Mittal, J. Fan, A. Migdall, and J. M. Taylor, “Imaging topological edge states in silicon photonics,” Nat. Photonics **7**, 1001 (2013).
13. S. Mittal, J. Fan, S. Faez, A. Migdall, J. M. Taylor, and M. Hafezi, "Topologically Robust Transport of Photons in a Synthetic Gauge Field," Phys. Rev. Lett. **113**, 087403 (2014).
14. X. Cheng, C. Jouvaud, X. Ni, S. H. Mousavi, A. Z. Genack, and A. B. Khanikaev, “Robust reconfigurable electromagnetic pathways within a photonic topological insulator,” Nat. Mater. **15**, 542 (2016).
15. V. Peano, M. Houde, F. Marquardt, and A. A. Clerk, "Topological Quantum Fluctuations and Traveling Wave Amplifiers," Phys. Rev. X **6**, 041026 (2016).
16. A. P. Slobozhanyuk, A. B. Khanikaev, D. S. Filonov, D. A. Smirnova, A. E. Miroshnichenko, and Y. S. Kivshar, "Experimental demonstration of topological effects in bianisotropic metamaterials," Sci. Rep. **6**, 22270 (2016).
17. M. Aidelsburger, M. Lohse, C. Schweizer, M. Atala, J. T. Barreiro, S. Nascimbène, N. R. Cooper, I. Bloch, and N. Goldman, “Measuring the Chern number of Hofstadter bands with ultracold bosonic atoms,” Nat. Phys. **11**, 162 (2015).
18. G. Jotzu, M. Messer, R. Desbuquois, M. Lebrat, T. Uehlinger, D. Greif, and T. Esslinger, “Experimental realization of the topological Haldane modelwith ultracold fermions,” Nature **515**, 237 (2014).
19. L. M. Nash, D. Kleckner, A. Read, V. Vitelli, A. M. Turner, and W. T. M. Irvine, “Topological mechanics of gyroscopic metamaterials,” Proc. Natl. Acad. Sci. **112**, 14495 (2015).
20. Z. Yang, F. Gao, X. Shi, X. Lin, Z. Gao, Y. Chong, and B. Zhang, "Topological Acoustics," Phys. Rev. Lett. **114**, 114301 (2015).
21. P. Wang, L. Lu, and K. Bertoldi, "Topological Phononic Crystals with One-Way Elastic Edge Waves," Phys. Rev. Lett. **115**, 104302 (2015).

22. C. L. Kane and T. C. Lubensky, “Topological boundary modes in isostatic lattices,” Nat. Phys. **10**, 39 (2013).
23. Y. C. Hu and T. L. Hughes, "Absence of topological insulator phases in non-Hermitian PT-symmetric Hamiltonians," Phys. Rev. B **84**, 153101 (2011).
24. K. Esaki, M. Sato, K. Hasebe, and M. Kohmoto, "Edge states and topological phases in non-Hermitian systems," Phys. Rev. B **84**, 205128 (2011).
25. M. Rudner and L. Levitov, "Topological Transition in a Non-Hermitian Quantum Walk," Phys. Rev. Lett. **102**, 065703 (2009).
26. J. M. Zeuner, M. C. Rechtsman, Y. Plotnik, Y. Lumer, S. Nolte, M. S. Rudner, M. Segev, and A. Szameit, "Observation of a Topological Transition in the Bulk of a Non-Hermitian System," Phys Rev Lett **115**, 40402 (2015).
27. S. D. Liang and G. Y. Huang, “Topological invariance and global Berry phase in non-Hermitian systems,” Phys. Rev. A **87**, 012118 (2013).
28. S. Weimann, M. Kremer, Y. Plotnik, Y. Lumer, S. Nolte, K. G. Makris, M. Segev, M. C. Rechtsman, and A. Szameit, “Topologically protected bound states in photonic parity–time-symmetric crystals,” Nat. Mater. **1**, 433 (2016).
29. H. Zhao, P. Miao, M. H. Teimourpour, S. Malzard, R. El-Ganainy, H. Schomerus, and L. Feng, "Topological Hybrid Silicon Microlasers," ArXiv170902747 Phys. (2017).
30. L. Pilozzi and C. Conti, "Topological lasing in resonant photonic structures," Phys. Rev. B **93**, 195317 (2016).
31. P. St-Jean, V. Goblot, E. Galopin, A. Lemaître, T. Ozawa, L. L. Gratiet, I. Sagnes, J. Bloch, and A. Amo, “Lasing in topological edge states of a one-dimensional lattice,” Nat. Photonics **11,** 651 (2017).
32. M. Parto, S. Wittek, H. Hodaei, G. Harari, M. A. Bandres, J. Ren, M. C. Rechtsman, M. Segev, D. N. Christodoulides, and M. Khajavikhan, "Complex Edge-State Phase Transitions in 1D Topological Laser Arrays," ArXiv170900523 Phys. (2017).
33. B. Bahari, A. Ndao, F. Vallini, A. E. Amili, Y. Fainman, and B. Kanté, "Nonreciprocal lasing in topological cavities of arbitrary geometries," Science eaao4551 (2017).
34. M. Segev, Y. Silberberg, and D. Christodoulidies, “Anderson localization of light,” Nat. Photonics **7**, 197 (2013).
35. J. Liu, P. D. Garcia, S. Ek, N. Gregersen, T. Suhr, M. Schubert, J. Mørk, S. Stobbe, and P. Lodahl, “Random nanolasing in the Anderson localized regime.,” Nat. Nanotechnol. **9**, 285 (2014).
36. F. D. M. Haldane, “Model for a quantum hall effect without landau levels: Condensed-matter realization of the “parity anomaly,”" Phys. Rev. Lett. **61**, 2015 (1988).
37. S. Mittal, S. Ganeshan, J. Fan, A. Vaezi, and M. Hafezi, "Measurement of topological invariants in a 2D photonic system," Nat. Photonics **10**, 180–183 (2016).
38. L. Feng, Z. Wong, R. Ma, Y. Wang, and X. Zhang, "Single-mode laser by parity-time symmetry breaking," Science **346**, 972 (2014).
39. H. Hodaei, M. Miri, M. Heinrich, D. N. Christodoulides, and M. Khajavikhan, "Parity-time–symmetric microring lasers," Science **346**, 975 (2014).
40. D. Liu, B. Zhen, L. Ge, F. Hernandez, A. Pick, S. Burkhardt, M. Liertzer, S. Rotter, and S. G. Johnson, “Symmetry, stability, and computation of degenerate lasing modes,” Phys. Rev. A **95**, 023835 (2016).
41. G. Q. Liang and Y. D. Chong, "Optical Resonator Analog of a Two-Dimensional Topological Insulator," Phys. Rev. Lett. **110**, 203904 (2013).

Figure 1

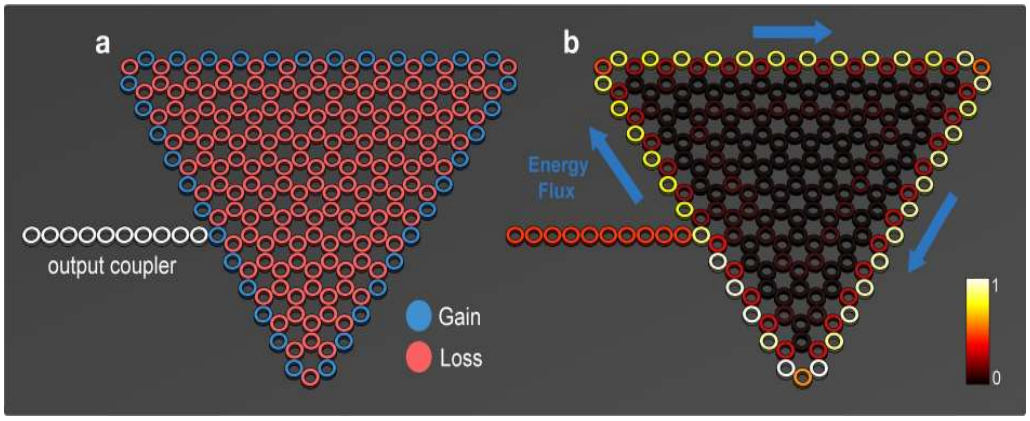

Figure 1 | The geometry and the lasing mode in a topological insulator laser based on the Haldane model. (a) Cavity geometry (same for topological and trivial): a planar honeycomb lattice of coupled microring resonators. The cavity has unpumped (lossy) resonators (red), pumped resonators (blue) and an output channel (white). (b) The steady state topological lasing mode of the topological cavity. The lasing mode is extended all around the perimeter of the cavity with almost-uniform intensity, and its energy flux is unidirectional. The unidirectional energy flux can be noticed by the intensity buildup as the mode circulates (clockwise), and by the sudden drop in intensity when passing (clockwise) the output coupler.

Figure 2

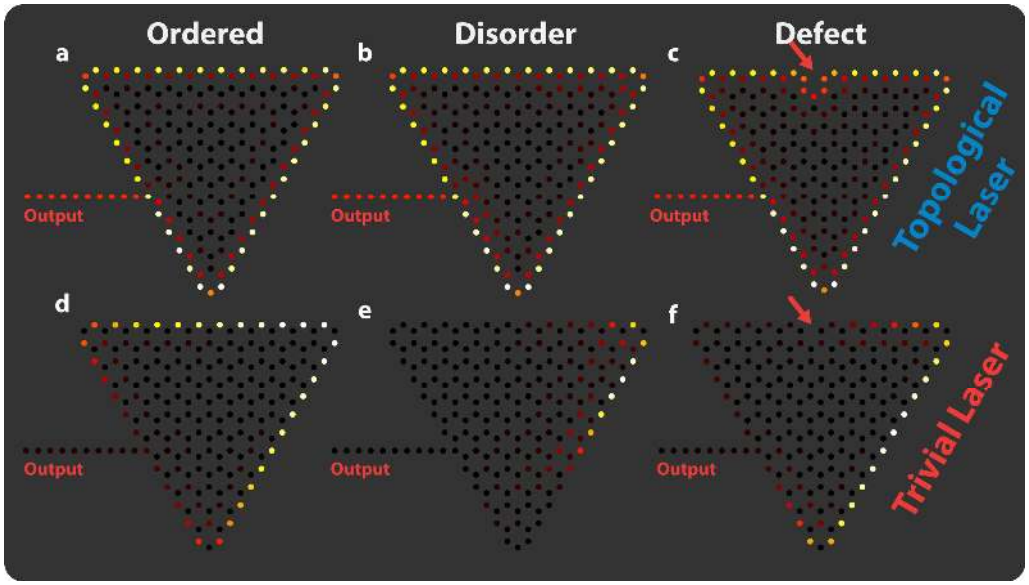

Figure 2 | Lasing modes in the topological and the trivial cavities (Haldane model). The panels show the steady state lasing modes (colors indicate amplitude) for the topological and trivial cavities with (a,d) no disorder, (b,e) disorder, and (c,f) a defect (a missing gain resonator at the perimeter). Being unidirectional and extended, with almost-uniform intensity, the lasing mode in the topological cavity (a-c) exhausts all the pumped sites and couples strongly to the output coupler in all cases. The trivial cavity, lacking unidirectional extended lasing modes, couples weakly to the output coupler even without disorder (d). The presence of disorder (e) and defects (f) make the lasing mode of the trivial cavity highly localized, reducing the efficiency further.

Figure 3

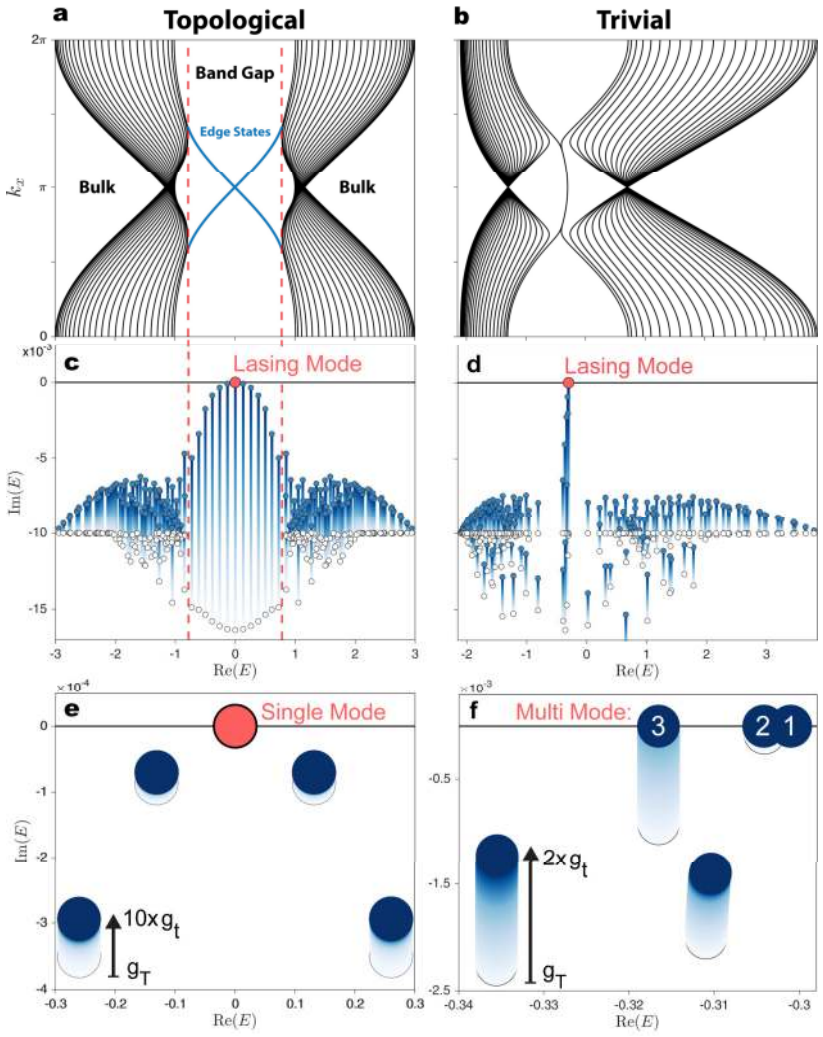

Figure 3 | The lasing process in the topological and the trivial laser cavities. (a-b) Band diagram of the passive (no gain or loss) (a) topological and (b) trivial strip of resonators. The topological cavity has a bandgap with topologically-protected unidirectional edge states crossing the gap (blue lines). On the other hand, the trivial cavity has no protected transport, as there is no gap and the edge states are degenerate. (c-d) The evolution of the real and imaginary part of the spectrum of the (c) topological and the (d) trivial cavities, from zero gain (white dots) up to the threshold gain (blue dots), which is where the first lasing mode lases. (e-f) Evolution of the spectrum of the laser cavity modes as the gain is increased further above the threshold gain. The topological laser (e) maintains single mode lasing, at least up to gain values of ten times the threshold gain. On the other hand, the trivial laser (f) becomes multimode, with three lasing modes, at a gain level just twice the threshold gain.

Figure 4

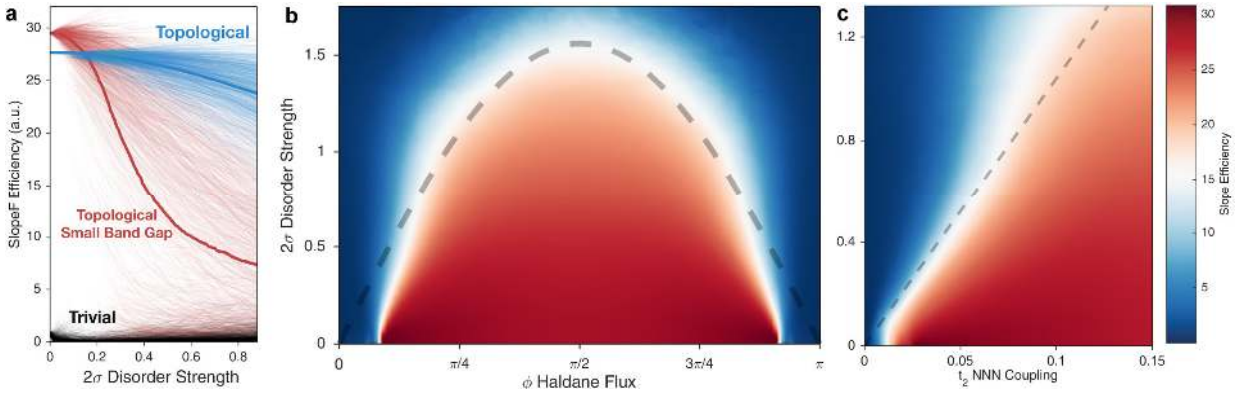

Figure 4 | Slope efficiency vs. disorder in the topological and the trivial laser systems (Haldane model). (a) The slope efficiency versus disorder strength (measured in terms of its standard deviation), for the topological laser with the maximum gap (blue; $\phi = \pi/2$), with a small topological gap (red; $\phi = \pi/8$), and for the trivial-laser with no gap (black; $\phi = 0$). Every point corresponds to the slope efficiency of a different realization of the disorder (1,000 in total). Solid lines mark the mean values for each case. The topological cavities exhibit higher slope efficiency (blue line) than the trivial cavity, even under high levels of disorder. For the topological insulator laser with a small band gap, when the disorder level is increased to above the band gap size, the topological protection of this topological laser starts to break and its efficiency is deteriorated dramatically (red line). (b-c) The mean value of the slope efficiency (average over 1,000 realization) as a function of (b) disorder and the Haldane flux (ϕ), and (c) disorder and second nearest neighbors coupling (t_2). The dotted black line in (b-c) depicts the size of the band gap of the Haldane model at zero disorder, given by $6\sqrt{3}t_2 \sin(\phi)$. Clearly, the slope efficiency of the topological cavity stays high as long as the disorder strength is lower than the size of the topological gap.

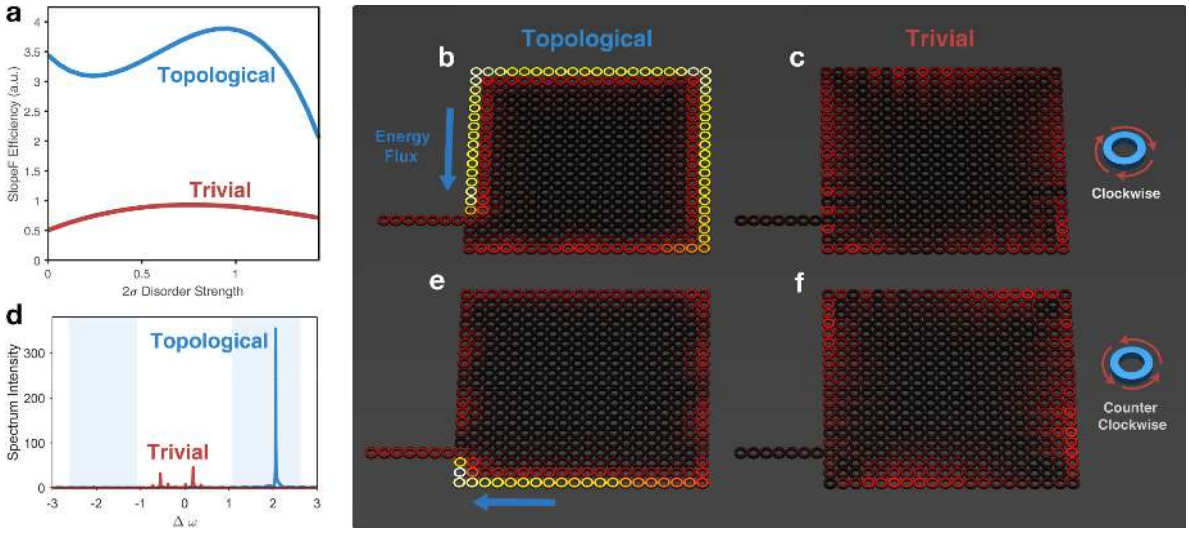

Figure 5 | Lasing modes in the topological and the trivial cavities (coupled resonators model). (a) Mean slope efficiency as a function of disorder strength (measured in terms of the standard deviation of the on-site energy) for the topological laser (blue) and the trivial laser (red). The simulation includes 5% backscattering on each site. The slope efficiency of the topological laser is higher and more robust up to disorder levels of the order of the topological bandgap. (b,c,e,f) Typical lasing modes (colors indicate amplitude) for the topological (b,e) and the trivial (c,f) cavities. The first/second row shows the CW/CCW components, respectively. In the topological array the CW (b) and CCW (f) components travel in opposite directions around the lattice but they both lase at the same frequency, synergistically transporting energy from the pumped sites to the output coupler. On the other hand, in the trivial lattice (c,f) the modes become localized in the presence of disorder, penetrate into the lossy bulk and couple only weakly to the output coupler. (d) The spectra of the topological (blue) and the trivial (red) lasers, for the same level of pumping. Even in the presence of disorder and backscattering, the topological array lases in a single mode inside one of the topological band gaps (shaded blue regions), whereas the trivial array, for the same gain and disorder levels, lases weakly and at multiple frequencies.

Supplementary Information for
Topological Insulator Lasers Part I: Theory

Haldane model: geometry and equations of motion

The Haldane model[1] employs a honeycomb lattice, with magnetic field that has zero average flux and maintains all the spatial symmetries of the lattice. The dynamics in this model is described by the real nearest-neighbor (nn) coupling coefficient, and, in addition, a complex next-nearest-neighbor (nnn) coupling coefficient that opens a topological bandgap by lifting the degeneracy at the Dirac points. Similar to the ordinary honeycomb lattice, the Haldane model can be described using the unit cell of a two-dimensional triangular lattice (with indices n, m) with a sub-basis of two sites, A and B. The equations of motion are:

$$i\frac{d}{dt}a_{nm} = \omega_0 a_{nm} + t_1 \sum_{\langle n.n.\rangle} b_{kl} + t_2 \sum_{\langle n.n.n\rangle} a_{kl} e^{i\phi_{kl}} \quad (1)$$

$$i\frac{d}{dt}b_{nm} = \omega_0 b_{nm} + t_1 \sum_{\langle n.n.\rangle} a_{kl} + t_2 \sum_{\langle n.n.n\rangle} b_{kl} e^{-i\phi_{kl}} \quad (2)$$

With $a_{nm}(b_{nm})$ being the amplitude at the n, m A (B) site, ω_0 the resonance frequency of resonator nm, nn is nearest neighbor with coupling coefficient t_1, nnn is next nearest neighbor with coupling coefficient t_2, and the flux $\phi_{kl} = \pm\phi$ is alternating between adjacent second nearest neighbors ($\phi \in [-\pi, \pi]$).

The topological transition occurs when $t_2 \neq 0$, where a topological bandgap is formed. The size of the topological bandgap is $6\sqrt{3}t_2 \sin\phi$, i.e. it is determined by the value of the nnn hopping constant and by the Haldane flux.

Realization of topological insulator lasers using semiconductor laser technology

Consider an array of coupled semiconductor laser cavities arranged in a square lattice of microring resonators ("rings") coupled via aperiodic linking resonators ("links"). The links are off-resonant with the rings so that light mostly inhibits the rings. In addition, the links are arranged in an aperiodic way, such that a vertically-dependent phase is picked for horizontal hopping, as seen in Fig. S1(a). In passive systems (no gain nor loss), this realization was proposed and demonstrated by Hafezi et. al.[2,3], who experimentally demonstrated that the system can be effectively described as a lattice of rings under the influence of a uniform out-of-plane magnetic field.

Here, we use this system in the presence of gain and loss, as shown in Fig. S1(b). This makes the system non-Hermitian, which means that the topological invariants are no longer defined, and therefore the presence of topological protection of transport is not naturally expected, in contrast with the passive case[2,3] where edge transport is always expected to be topologically-protected.

To promote the lasing of the topological edge modes, the sites on the perimeter are pumped, thereby exhibiting gain (blue), while the interior sites are lossy (red). The light exits the cavity the output coupler, which consists of a semi-infinite one dimensional lattice of transparent sites (white). The links between adjacent rings are transparent (no gain nor loss). As suggested earlier[2,3], we effectively describe the system by omitting the links, as seen in Fig. S1(c), and making the ring-ring coupling coefficients complex.

As explained in the main text, the linear system is reciprocal, hence every ring supports clockwise (CW) and counterclockwise (CCW) modes. Figure S2(a-b) shows the band diagram of this system (calculated on an infinite strip) for the topological and the trivial phases, respectively, where the ring resonators are excited to circulate in a clockwise manner only. The topological phase has a $\pi/2$ flux and supports two topological gaps. Each topological bandgap supports circulation of edge modes in both directions. That is, in the upper topological gap, the upper (red) and the lower (green) edge states circulate CW, while in the lower gap they circulate CCW. In addition, there are edge states with frequencies in a bulk band. Figure S2(c) shows the band diagram of the other case, where all the resonators are excited in a CCW mode only.

In a passive linear system[2,3], the CW and the CCW can be coupled only through scattering from defects and imperfections. In this sense, the strength of the coupling directly relates to the level of disorder in the system, which realistically – in state of the art technology of semiconductor lasers – is not more than a few percent. In other words, the coupling between neighboring resonators can be made sufficiently strong that intrinsic fabrication disorder is relatively weak. However, lasers are fundamentally highly nonlinear systems, because lasing inherently relies on gain saturation. For this reason, the simulations here include both linear CW-CCW coupling via backscattering, and nonlinear coupling via on-site saturation of the gain/loss in every resonator. In principle, in a linear passive system backscattering would ruin the topological protection and the edge states would no longer be unidirectional, impairing the protected topological transport. Here, we show that the protected topological transport is

restored due to the laser action and the nonlinear nature of gain/loss saturation. The modified equations governing the dynamics are therefore[4–6]

$$i\dot{a}_{nm} = \left(\omega_0 + \Delta_{nm} + \frac{ig\mathbb{P} - ig_{max}(1-\mathbb{P})}{1+(|a_{nm}|^2+|b_{nm}|^2)/I_{sat}} - i\gamma_0\right) a_{nm} + ta_{n\pm1l}e^{\pm i\phi l} + ta_{nl\pm1} + t_{BS}b_{nm} \tag{3}$$

$$i\dot{b}_{nm} = \left(\omega_0 + \Delta_{nm} + \frac{ig\mathbb{P} - ig_{max}(1-\mathbb{P})}{1+(|a_{nm}|^2+|b_{nm}|^2)/I_{sat}}\mathbb{P} - i\gamma_0\right) b_{nm} + tb_{n\pm1l}e^{\mp i\phi l} + tb_{nl\pm1} + t_{BS}a_{nm} \tag{4}$$

With $a_{nm}(b_{nm})$ being the amplitude of the CW (CCW) mode at the n,m site, ω_0 the on-site resonator frequency, Δ_{nm} disorder term (shift of the resonance frequency of the resonator at site n,m), g the gain in the system (depending on the pump intensity can be as high as g_{max},), I_{sat} the gain saturation intensity, $\mathbb{P}$ the pump profile (i.e, equals unity when pumped and 0 when not pumped), γ_0 residual ring loss, t the coupling coefficient, ϕ the coupling phase ($\pi/2$ for the topological phase and 0 for the trivial phase; note the opposite sign for CW and CCW modes) , t_{BS} the backscattering coupling coefficient.

We emphasize that despite the complexity of the setting, wherein two circulating cavity modes can exist simultaneously and interact through the nonlinearity (saturation) and backscattering, our analysis and simulations show that the lasing modes are the topological modes, i.e., their frequencies are in the topological bandgaps, and they exhibit topologically-protected transport. This is highlighted by Fig. 5 of the main text, where we show that the topological laser system has a considerably higher slope efficiency than the trivial one, for disorder up to the level that is comparable to the topological bandgap. We have observed that for disorder amplitude below the size of approximately twice the coupling constant the system is robust, with extended topological edge modes, resulting in single-mode highly efficient lasing. It is only when the disorder level exceeds the size of the gap (~ twice the coupling coefficient), that the presence of disorder diminishes the topological bandgap and the laser loses its superior features.

Comparison to perimeter-only geometries

It is instructive to compare the realization of the topological insulator laser based on semiconductor laser technology (described in the previous section) to the following two geometries: (1) a large single ring with the same perimeter length as the topological cavity,

and (2) an array of micro-rings situated along the perimeter only, without the interior bulk lossy sites.

The single ring cavity supports multiple, narrowly spaced, longitudinal modes with similar quality factors, and hence lases in a multi-mode manner even close to the threshold gain. This feature was one of the main drivers to turn to arrays of single-mode micro-ring resonators[4] for photonic integrated circuits, where stability of the lasing frequency is important.

The second case, of an array of microring resonators positioned along the perimeter-only, consisting of only the pumped sites while the lossy bulk sites are removed, shows the importance of the topological lattice to stabilize the lasing mode. In the topological lattice, the lasing mode inherits the topological features of the lattice, manifested in a unidirectional and robust topologically protected lasing mode. On the other hand, in the perimeter-only case, the lattice is highly susceptible to disorder and defects, causing multi-mode lasing and weak coupling to the output coupler. To explain this on intuitive footing, when disorder (or a defect) is introduced into the perimeter-only setting, the light cannot bypass the defect by propagating around it through the bulk. Instead, a defect in the perimeter-only setting will decouple the sites on either side, and multiple defects result in lasing in multiple localized modes simultaneously. In the linear limit, this behavior can be understood as arising from Anderson localization.

To conclude, to role of the topological construction is vital for the efficient and stable operation of the laser. Even if we consider a simpler geometry such as a large ring, or if we eliminate the lossy bulk sites altogether, the fact that the topological cavity lases cooperatively in a unidirectional topologically-protected mode, which is protected against localization, makes the topological insulator laser much more efficient and stable, with very high output power in a desirable narrow-band single mode.

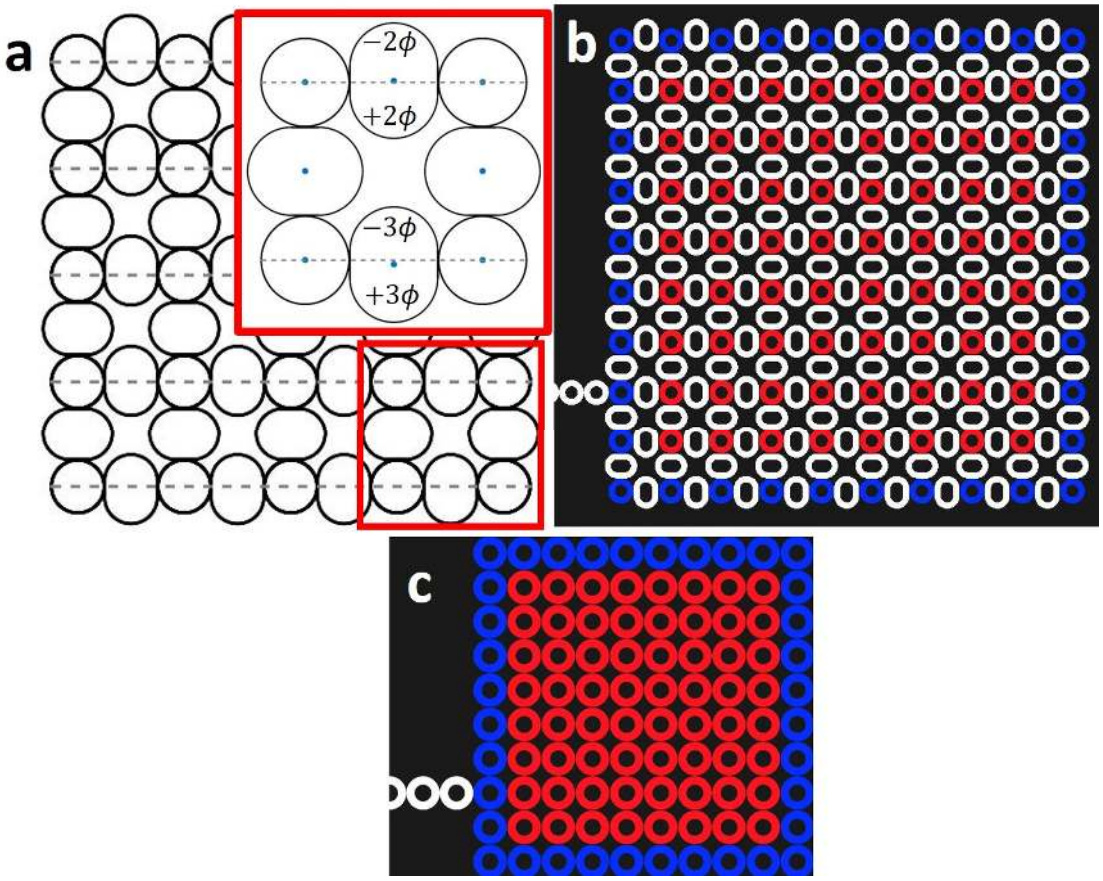

Figure S1: **Geometry and pumping profile of the experimental model.** (a) Top view of the lattice, consisting of ring and link resonators. The rings are coupled via the off-resonance links. The links that induce horizontal hoping between rings are vertically shifted, yielding an overall phase when going around a plaquette, as seen in the inset. (b) The pumping scheme of the entire structure, and (c) the effective description of the lattice.

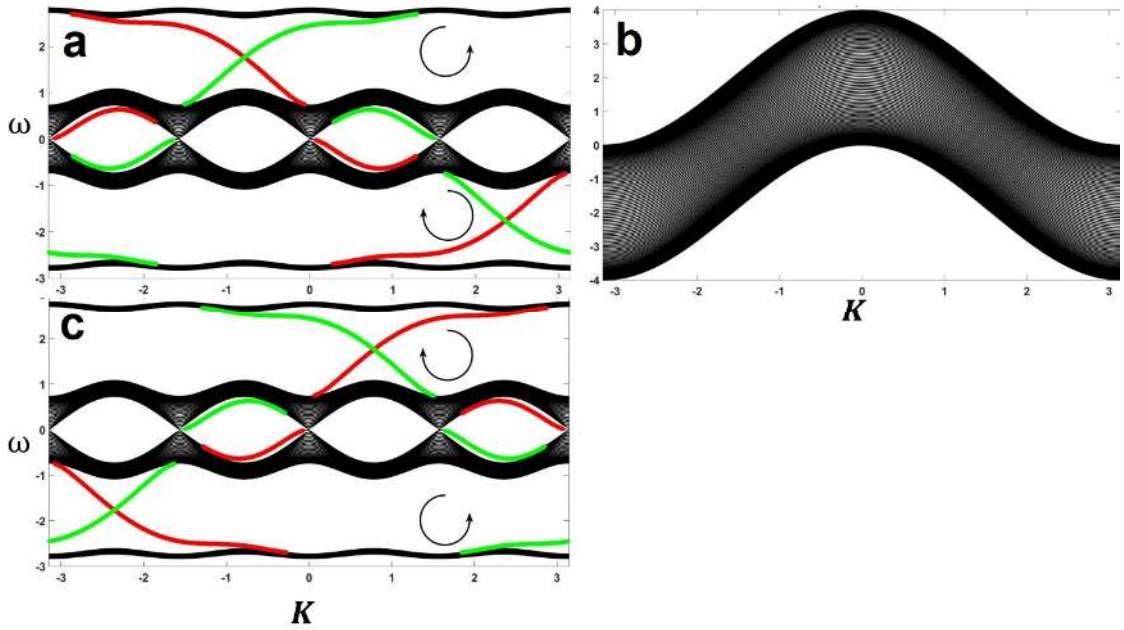

Figure S2: **Band diagram of the model based on an all-dielectric aperiodic array of resonators**. (a),(c) Band diagrams of the topological structure with $\pi/2$ $(-\pi/2)$ flux (same value as the topological phase in the main text), corresponding to the CW and CCW resonator modes, respectively. The edge states of the upper (red) and lower (green) edges reside in the topological gaps. The circulation in each gap is indicated by the circling arrows. For different lasing frequencies the circulation direction changes. (b) band-diagram of the trivial phase (created by placing the links symmetrically), showing that there are no bandgaps and no edge states.

References

1. Haldane, F. D. M. Model for a quantum hall effect without landau levels: Condensed-matter realization of the 'parity anomaly'. *Phys. Rev. Lett.* **61,** 2015–2018 (1988).

2. Hafezi, M., Demler, E., Lukin, M. & Taylor, J. Robust optical delay lines via topological protection. *Nat. Phys.* **7,** 9 (2011).

3. Hafezi, M., Mittal, S., Fan, J., Migdall, A. & Taylor, J. M. Imaging topological edge states in silicon photonics. *Nat. Photonics* **7,** 1001–1005 (2013).

4. Yariv, a, Xu, Y., Lee, R. K. & Scherer, a. Coupled-resonator optical waveguide: a proposal and analysis. *Opt. Lett.* **24,** 711–713 (1999).

5. Poon, J. K. S. *et al.* Matrix analysis of microring coupled-resonator optical waveguides. *Opt. Express* **12,** 90–103 (2004).

6. Hodaei, H., Miri, M., Heinrich, M., Christodoulides, D. N. & Khajavikhan, M. Parity-time–symmetric microring lasers. *Science* **346,** 975 (2014).